Journal of Veterinary Cardiology (2025) **59**, 93—97

Journal of Veterinary Cardiology
ESVC

www.elsevier.com/locate/jvc

Cardiovascular Images

Left atrial thrombosis in a dog with advanced myxomatous mitral valve disease☆

G. Romito*, C. Mazzoldi, M. Di Benedetto, S. Sabattini

Department of Veterinary Medical Sciences, Alma Mater Studiorum - University of Bologna, via Tolara di Sopra 50, 40064 Ozzano dell'Emilia, Italy

Received 24 May 2024; received in revised form 9 March 2025; accepted 28 March 2025

KEYWORDS
Canine;
Jet lesion;
Left atrial rupture;
Atrial septal defect;
Intracardiac thrombosis

Abstract An 11-year-old Cavalier King Charles spaniel with a previous diagnosis of preclinical myxomatous mitral valve disease (MMVD) was presented with respiratory distress and abdominal distension. Lung edema and ascites were diagnosed. Echocardiography revealed a progression of the MMVD as it was associated with a moderate enlargement of the left-sided cardiac chambers and an atrial septal defect (ASD). The latter was hypothesized to be primarily due to a rupture of the interatrial septum caused by MMVD. Moreover, a hyperechoic irregular mass was documented inside the left atrium. At that time, the primary differential diagnosis included intracardiac thrombosis (ICT) and mural endocarditis. Comprehensive diagnostic tests subsequently ruled out extracardiac prothrombotic triggers; moreover, both blood and urine cultures tested negative. Despite the administration of cardiac and supportive therapies (including antithrombotic drugs), the dog died 138 days after presentation. Necropsy confirmed the presence of MMVD (type IV lesions according to Pomerance and Whitney's classification system) associated with remodeling of the left-sided cardiac chambers, multiple left atrial (LA) jet lesions, and ASD. Endocarditis was ruled out, and the LA mass was demonstrated to be an ICT entrapped in the ASD. In light of premortem and postmortem findings, the turbulent blood flow secondary to the mitral valve insufficiency and ASD, along with the extensive LA endothelial damage, were considered likely triggering factors

☆ A unique aspect of the Journal of Veterinary Cardiology is the emphasis on additional web-based images permitting the detailing of procedures and diagnostics. These images can be viewed (by those readers with subscription access) by going to http://www.sciencedirect.com/science/journal/17602734. The issue to be viewed is clicked and the available PDF and image downloading is available via the Summary Plus link. The supplementary material for a given article appears at the end of the page. Downloading the videos may take several minutes. Readers will require at least Quicktime 7 (available free at http://www.apple.com/quicktime/download/) to enjoy the content. Another means to view the material is to go to http://doi.org/10.1016/j.jvc.2025.03.009.

* Corresponding author.
E-mail address: giovanni.romito2@unibo.it (G. Romito).

https://doi.org/10.1016/j.jvc.2025.03.009

for the development of ICT. This case suggests that, although ICT represents an extremely rare complication of cardiac diseases in dogs, it can potentially develop when canine MMVD is particularly advanced.

Abbreviations

ASD	atrial septal defect
IAS	interatrial septum
ICT	intracardiac thrombosis
LA	left atrial
MMVD	myxomatous mitral valve disease

An 11-year-old, 9.5-kg Cavalier King Charles spaniel was referred for respiratory distress and abdominal distension. The past medical history included only stage B2 myxomatous mitral valve disease (MMVD). At the last echocardiographic examination (performed nine months earlier), this was not associated with any additional cardiological abnormalities, apart from the typical changes related to the mitral valve (i.e. mitral valve thickening and prolapse). At that time, pimobendan was prescribed. Over the following months, the dog did not receive any additional cardiovascular drugs. Upon presentation, physical abnormalities included grade IV/VI left apical and III/VI right apical holosystolic murmurs, abdominal distension with a palpable fluid wave, and respiratory effort with audible pulmonary crackles. Electrocardiogram revealed sinus tachycardia (180 beats/min). Thoracic radiographs documented pulmonary edema. A focused abdominal ultrasound examination showed severe effusion and caudal vena cava congestion. Transthoracic echocardiography[a] was also performed.

Image interpretation

Echocardiography

Two-dimensional analysis revealed severe thickening and prolapse of the atrioventricular valves, moderate enlargement of the left-sided cardiac chambers (left atrium-to-aortic root ratio: 2.1; left atrial [LA] anteroposterior diameter: 49 mm; left ventricular end-diastolic and end-systolic volume index: 134 mL/m^2 and 34 mL/m^2, respectively), subjectively mild enlargement of the right-sided cardiac chambers, an atrial septal defect (ASD), which was strongly suspected to be acquired given its absence on previous examinations, and a hyperechoic irregular mass with the proximal portion apparently entrapped in the ASD and the distal one protruding inside the LA cavity. Doppler analysis documented severe mitral regurgitation, part of which impacted the interatrial septum (IAS), moderate tricuspid regurgitation (peak systolic velocity: 3.4 m/s [estimated right ventricular-to-right atrial pressure gradient: 46 mmHg]), a left-to-right intracardiac shunting flow across the ASD (peak velocity: approximately 3 m/s; estimated LA-to-right atrial pressure gradient: 36 mmHg), and elevated left ventricular filling pressures (E wave peak velocity: 1.6 m/s; E/isovolumic relaxation time: 3.5) (Figs 1 and 2, Video 1).

The dog was hospitalized for the management of congestive heart failure and initially treated with intravenous furosemide, oral pimobendan, oxygen supplementation, and abdominocentesis. Since the differential diagnosis for the LA mass primarily included intracardiac thrombosis (ICT) and mural endocarditis, comprehensive laboratory tests (complete blood count, serum biochemistry, coagulation panel, urinalysis with proteinuria, urine culture, and blood cultures from separate venipuncture sites) and a complete abdominal ultrasound were performed during hospitalization. Pending results, antithrombotic (clopidogrel [4 mg/kg PO q 24 h] and enoxaparin [1 mg/kg subcutaneously (SC) q 12 h]) and antibiotic therapy (ampicillin-sulbactam [20 mg/kg intravenously (IV) q 12 h] and marbofloxacin [3 mg/kg IV q 24 h]) were empirically started. Over the next days, no extracardiac prothrombotic conditions were demonstrated; cultures tested negative.

After discharge, serial controls were performed constantly showing the LA mass. Relapses of bilateral congestive heart failure and the development of focal atrial tachycardia occurred over the following months. Accordingly, cardiac therapies were progressively modified and finally

[a] iU22 ultrasound system, Philips Medical Systems S.p.A., Monza, Italy.

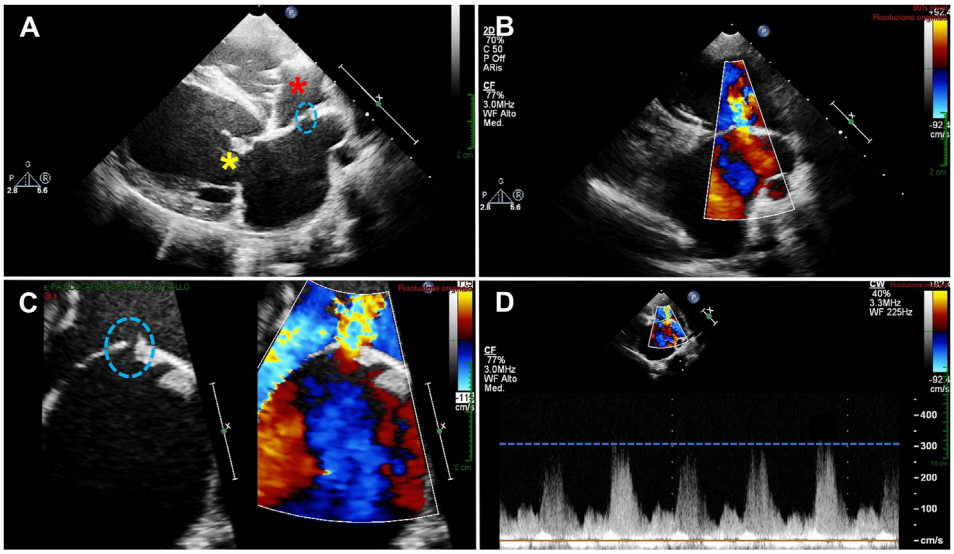

Figure 1 (A) Two-dimensional right parasternal long-axis four-chamber view. Note the irregular thickening of the mitral valve leaflets (yellow asterisk), typical of myxomatous mitral valve degeneration, and the moderate enlargement of the left-sided cardiac chambers. Irregular thickening of the tricuspid valve leaflets (red asterisk) and a subjectively mild enlargement of the right-sided cardiac chambers can also be appreciated. Moreover, a small discontinuity of the interatrial septum can be noted (blue dotted circle). (B) Color flow Doppler analysis at the level of the interatrial septum obtained from a two-dimensional right parasternal long-axis four-chamber view. Note the intracardiac shunting flow moving from the left atrium to the right atrium through the aforesaid atrial septal defect. (C) Two-dimensional right parasternal short-axis view optimized for the visualization of the interatrial septum without and with color flow Doppler analysis. This view allows further appreciation of the discontinuity of the interatrial septum (blue dotted circle) and the intracardiac left-to-right shunting flow. (D) Spectral Doppler study of the intracardiac shunt due to the atrial septal defect. This image allows further appreciation of the direction of the shunting flow and estimation of the left atrial-to-right atrial pressure gradient (the blue dotted line shows the peak velocity of the shunting flow).

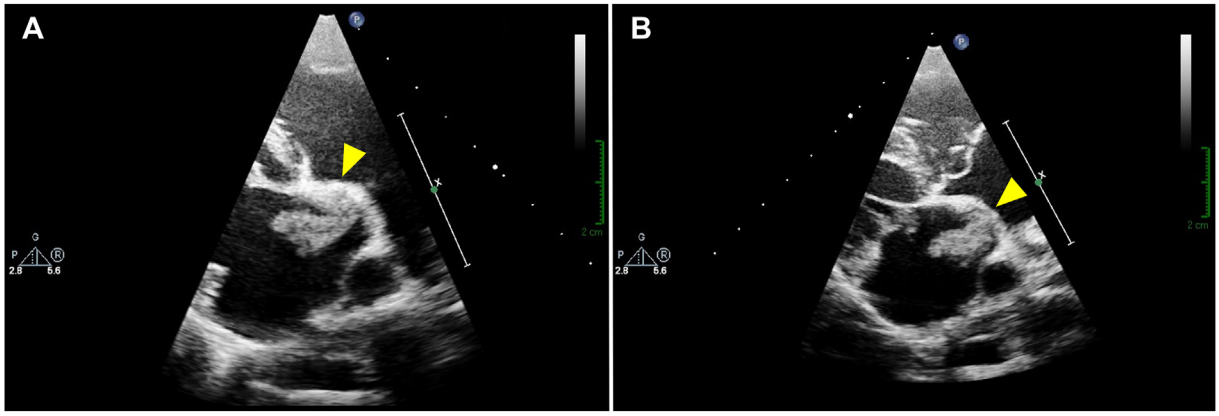

Figure 2 Two-dimensional right parasternal long-axis view optimized for visualization of the left atrial mass in different phases of the cardiac cycle (panel A: ventricular diastole; panel B: ventricular systole). In both panels, the left atrial mass appears as a hyperechoic, irregular lesion. Note that its proximal portion seems to be entrapped in the atrial septal defect in these optimized views (yellow arrowheads). Combining information from Figures 1 and 2, it was suspected that, at the time of acquisition of the echocardiographic images, the mass did not completely fill the atrial septal defect. Indeed, thanks to different echocardiographic probe angulations and rotations, it was possible to enhance the visualization of the patent part of the atrial septal defect and the intracardiac shunting flow (as shown in Fig. 1) or, alternatively, to enhance the visualization of the proximal portion of the mass entrapped in the defect (as shown in Fig. 2).

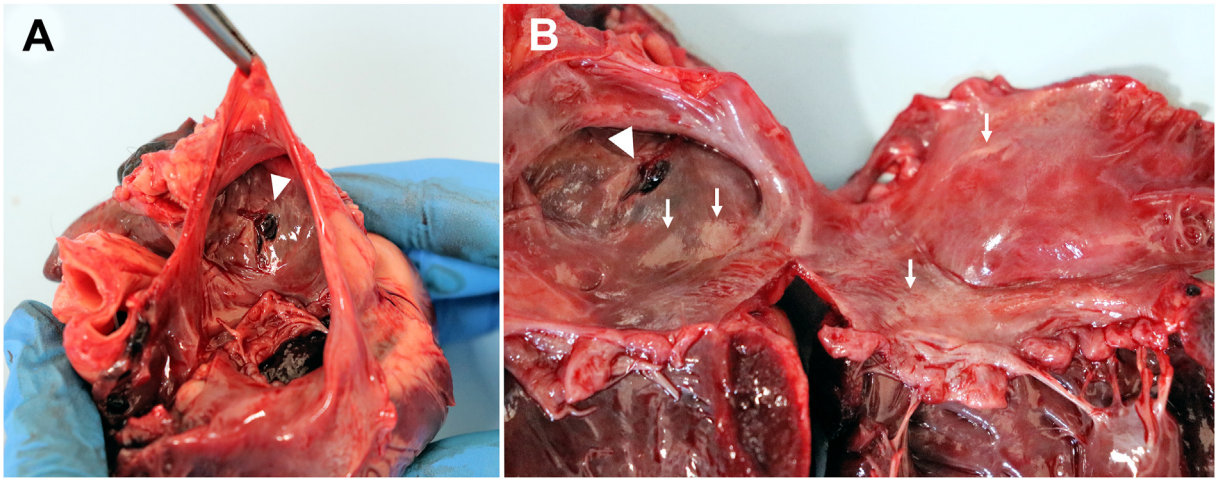

Figure 3 (A) Close-up of the interatrial septum viewed from the left side after dissection of the left atrial free wall. Approximately in the middle of the interatrial septum, a defect filled by a thrombus can be identified (white arrowhead). A large part of the thrombus was removed during necropsy to allow better examination of the interatrial septum; consequently, only its proximal portion, entrapped in the defect, is evident at this time. (B) Opened-out left-sided cardiac chambers. The defect is visible at the top-right side (white arrowhead), and multiple jet lesions (white arrows) can be seen. These appear as non-elevated, opaque gray streaks and plaques of variable size and depth. Some of them are closer to the defect, while others developed far from the interatrial septum. Pathological features of myxomatous mitral valve degeneration can also be identified. Note that the leaflet edges are rounded with variable and generally moderate-to-severe thickening and chordae tendineae are thickened.

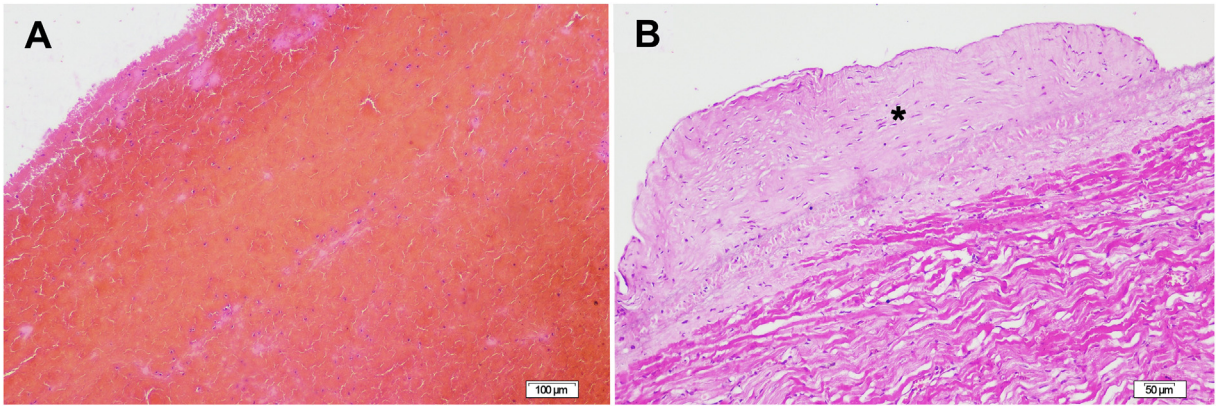

Figure 4 (A) Histological preparation of the left atrial mass. The mass is composed exclusively of red blood cells and fibrin, consistent with a thrombus. Hematoxylin and eosin staining. 100x magnification. Bar: 100 µm. (B) Histological preparation of a portion of the left atrium including one of the various jet lesions. The subendocardial tissue is focally expanded by an increased amount of collagen admixed with fibrocytes (fibrosis) (black asterisk). Hematoxylin and eosin staining. 100x magnification. Bar: 50 µm.

included torasemide (0.45 mg/kg PO q 12 h), pimobendan (0.35 mg/kg PO q 8 h), spironolactone (3 mg/kg PO q 24 h), hydrochlorothiazide (0.7 mg/kg PO q 12 h), and amiodarone (8 mg/kg PO q 24 h). Antithrombotic drugs were persistently administered (clopidogrel [unchanged dose] and rivaroxaban [0.9 mg/kg PO q 24 h]). Given the worsening of the dog's clinical condition, owners elected euthanasia (138 days after presentation) and consented to autopsy.

Necroscopic findings

Opening of the left atrium revealed a friable, irregular red mass (3.5 × 2.5 cm), which was adherent to the IAS and protruded in the LA cavity, consistent with a mural thrombus. Upon its removal, an irregular full-thickness perforation was noted in the middle of the IAS (0.6 × 1 cm). Multiple LA jet lesions were identified; some surrounded the IAS defect, while others were located far from it.

Mitral and tricuspid valves showed multiple nodular thickenings of various dimensions (type IV lesions according to Whitney's classification system [1]), consistent with endocardiosis. Histological examination confirmed MMVD and ICT and excluded endocarditis (Figs. 3 and 4). Given the antemortem and postmortem findings, an acquired ASD secondary to MMVD was strongly suspected.

Discussion

In dogs, ICT is an extremely rare complication of cardiac diseases. Previously, it was only described in a dog with mitral stenosis [2], three dogs with atrial fibrillation [3], a dog with infective endocarditis [4], a dog with suspected myocarditis [5], and a dog with rupture of the LA free wall leading to hemopericardium [6]. In contrast, no cases of ICT associated with a naturally acquired ASD due to MMVD were cited in veterinary literature. To date, reasons for the low propensity of dogs to the development of ICT are not completely known. In this case, we hypothesized that ICT developed primarily due to the endothelial damage caused by MMVD. Indeed, MMVD can generate high-velocity jets of mitral regurgitation that injure the LA endocardium, resulting in endocardial (jet) lesions. In severe cases as the present one, some of them can progress to full-thickness perforations of the LA walls[b] [7–9]. The pathophysiological association between the development of an ASD and the occurrence of ICT is also supported by reports on trans-septal catheterization. Indeed, ICT has been documented consequently to IAS rupture both in humans [10,11] and a dog [12] undergoing this interventional procedure.

Conflicts of Interest Statement

The authors do not have any conflicts of interest to disclose.

Supplementary data

Supplementary video related to this article can be found at https://doi.org/10.1016/j.jvc.2025.03.009.

Video	Title	Description
1	Close-up of a transthoracic echocardiographic video clip obtained from an optimized right parasternal long-axis four-chamber view.	The view has been optimized to help observe the left atrial mass features, including its location and size. This view also allows appreciation of moderate left atrial dilatation, subjectively mild right atrial dilatation, and thickening and prolapse of the atrioventricular valves.

References

[1] Pomerance A, Whitney JC. Heart valve changes common to man and dog: a comparative study. Cardiovasc Res 1970;4:61–6.

[2] Tashjian RJ, McCoy JR. Acquired mitral stenosis resulting in left atrial dilatation with thrombosis. A case report. Cornell Vet 1960;50:485–93.

[3] Usechak PJ, Bright JM, Day TK. Thrombotic complications associated with atrial fibrillation in three dogs. J Vet Cardiol 2012;14:453–8.

[4] Romito G, Cipone M. Infective endocarditis causing aorto-pulmonary fistula and intracardiac thrombosis in a dog. J Small Anim Pract 2020. https://doi.org/10.1111/jsap.13278.

[5] Caivano D, Birettoni F, Giorgi ME, Porciello F. What is your diagnosis? Intracardiac thrombus. J Am Vet Med Assoc 2014;245:1003–5.

[6] Caivano D, Marchesi MC, Birettoni F, Lepri E, Porciello F. Left atrial mural thrombosis and hemopericardium in a dog with myxomatous mitral valve disease. Vet Sci 2021;8:112.

[7] Buchanan JW. Spontaneous left atrial rupture in dogs. Adv Exp Med Biol 1972;22:315–34.

[8] Romito G, Testa F, Cipone M. Suspected sequential left atrial ruptures in a dog with myxomatous mitral valve disease. J Vet Cardiol 2022;44:18–22.

[9] Czech AA, Glaus TM, Testa F, Romito G, Baron Toaldo M. Clinical presentation, echocardiographic findings, treatment strategies, and prognosis of dogs with myxomatous mitral valve disease presented with pericardial effusion due to suspected left atrial tear: a retrospective case-control study. J Vet Cardiol 2024;51. 105–5.

[10] Lee JH, Kim JH, Choi JH, Kim EJ. Left atrial thrombus due to transseptal catheterization simulating solid mass of right atrium. J Cardiothorac Surg 2017;12:66.

[11] Okuyama T, Watanabe T, Harada K, Watanabe H, Yokota A, Kamioka M, Komori T, Kabutoya T, Imai Y, Kario K. Thrombus formation near the puncture site of the interatrial septum after second-generation cryoballoon ablation for paroxysmal atrial fibrillation. Circ J 2021;85:1401.

[12] Allen J, Phipps K, Barrett K. Transseptal puncture in the dog utilizing three-dimensional transesophageal echocardiographic guidance. J Vet Cardiol 2024;51:64–71.

[b] Buchanan JW. Chronic valve disease and left atrial splitting in the dog. Master's thesis, University of Pennsylvania; 1966.